

Synaptic potentiation onto habenula neurons in the learned helplessness model of depression

Bo Li^{1,2*}, Joaquin Piriz^{1*}, Martine Mirrione^{2,3*}, ChiHye Chung^{1*}, Christophe D. Proulx¹, Daniela Schulz³, Fritz Henn^{2,3} & Roberto Malinow¹

The cellular basis of depressive disorders is poorly understood¹. Recent studies in monkeys indicate that neurons in the lateral habenula (LHb), a nucleus that mediates communication between forebrain and midbrain structures, can increase their activity when an animal fails to receive an expected positive reward or receives a stimulus that predicts aversive conditions (that is, disappointment or anticipation of a negative outcome)^{2–4}. LHb neurons project to, and modulate, dopamine-rich regions, such as the ventral tegmental area (VTA)^{2,5}, that control reward-seeking behaviour⁶ and participate in depressive disorders⁷. Here we show that in two learned helplessness models of depression, excitatory synapses onto LHb neurons projecting to the VTA are potentiated. Synaptic potentiation correlates with an animal's helplessness behaviour and is due to an enhanced presynaptic release probability. Depleting transmitter release by repeated electrical stimulation of LHb afferents, using a protocol that can be effective for patients who are depressed^{8,9}, markedly suppresses synaptic drive onto VTA-projecting LHb neurons in brain slices and can significantly reduce learned helplessness behaviour in rats. Our results indicate that increased presynaptic action onto LHb neurons contributes to the rodent learned helplessness model of depression.

To study the cellular basis of behavioural depression, we examined the synaptic circuitry in the LHb of rats showing learned helplessness (Fig. 1), a model of depression whereby animals show reduced escape from escapable foot shock¹⁰. We used two well-established animal models: acute learned helplessness (aLH), which is induced by subjecting rats to periods of inescapable and unpredictable shock¹⁰; and congenital learned helplessness (cLH), which is present in a strain of rats produced by selective breeding of animals that show the greatest amount of aLH^{11,12}. In addition to showing reduced escape from escapable foot shock, animals with cLH and aLH also showed greater immobility in the forced swim test, another widely used animal model for depression¹³, than control animals (Fig. 2a, b).

We examined transmission onto LHb neurons. These neurons receive major inputs from numerous brain regions involved in stress response (such as the entopeduncular nucleus, lateral hypothalamus, lateral preoptic area, medial prefrontal cortex and the bed nucleus of the stria terminalis)¹⁴ (Supplementary Fig. 1) and can control dopaminergic function in the midbrain⁴. We wished to determine whether synaptic transmission onto LHb neurons is different in animals with learned helplessness and normal animals. To record selectively from LHb neurons that can regulate the activity of dopamine-producing neurons, we injected a retrograde tracer, cholera toxin conjugated to the dye Alexa Fluor 488, into the VTA *in vivo*. Two to three days later, we prepared brain slices that contained the LHb. A minority of neurons in the LHb were fluorescent, which indicated their projection to the VTA (Supplementary Fig. 2a, b). Notably, the LHb neurons that project to the VTA and to the rostromedial tegmental nucleus—a newly identified GABA (γ -aminobutyric acid)-producing, inhibitory relay station

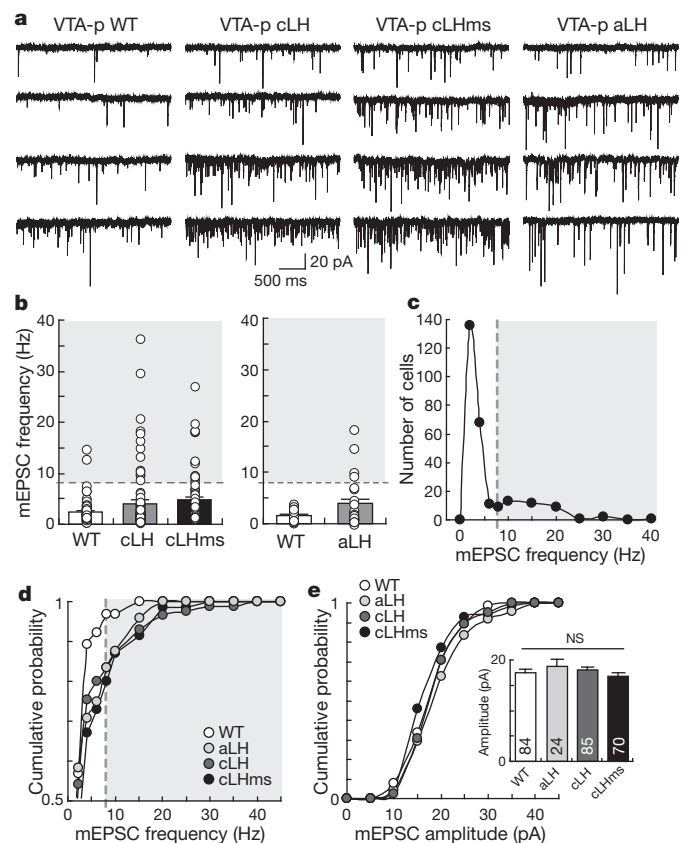


Figure 1 | Increased excitatory synaptic transmission onto VTA-projecting LHb neurons in the learned helplessness models of depression. **a**, Examples of mEPSCs recorded from VTA-projecting LHb neurons (VTA-p) from wild-type control (WT) animals and animals with cLH, cLHms or aLH. **b**, Means (histogram bars) and individual recordings (open circles) of mEPSC frequency from VTA-projecting LHb neurons in various groups of animals. Left: WT, 2.4 ± 0.3 , $n = 65$ (6 animals); cLH, 4.0 ± 0.7 , $n = 85$ (8 animals), $P < 0.05$ bootstrap method; cLHms, 4.7 ± 0.7 , $n = 70$ (8 animals), $P < 0.001$ bootstrap. Right: WT, 1.8 ± 0.2 , $n = 19$ (4 animals); aLH, 3.7 ± 0.8 , $n = 23$ (4 animals), $P < 0.05$ bootstrap. Results are presented as mean \pm s.e.m. P values are compared with WT group. Shaded region beyond dashed lines indicates high-frequency mEPSCs. n , number of cells. **c**, Frequency distribution of mEPSC frequencies of all cells recorded ($n = 263$ from 34 animals) showed bimodal distribution. **d**, The cumulative probability of mEPSC frequency of VTA-projecting LHb neurons in different groups of animals ($P < 0.05$, Kolmogorov–Smirnov (K–S) test comparing WT with any other group). **e**, The amplitude of mEPSCs did not differ among the four animal groups ($P > 0.3$, bootstrap). Inset shows mean \pm s.e.m. n , number of cells; NS, not significant.

¹Center for Neural Circuits and Behavior, Departments of Neuroscience and Biological Sciences, 9500 Gilman Drive # 0634, University of California at San Diego, La Jolla, California 92093, USA. ²Cold Spring Harbor Laboratory, 1 Bungtown Road, Cold Spring Harbor, New York 11724, USA. ³Brookhaven National Laboratory, Upton, New York 11973, USA.

*These authors contributed equally to this work.

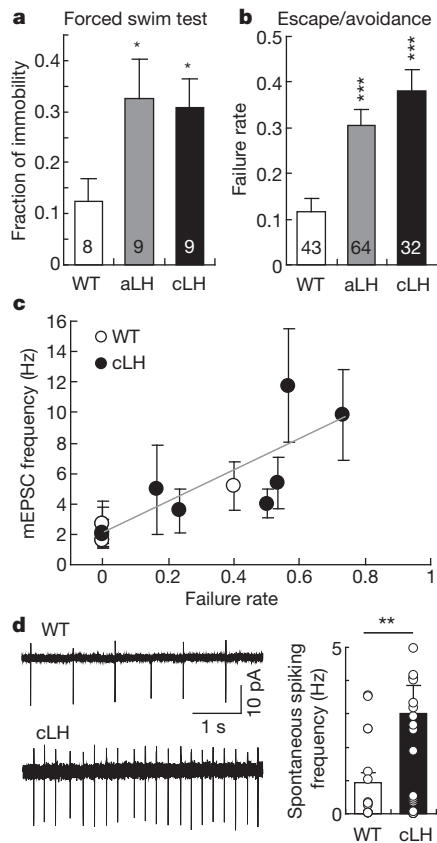


Figure 2 | Enhanced synaptic transmission onto VTA-projecting Lhb neurons correlates with helpless behaviour of individual animals.

a, b, Animals with aLH or cLH show behavioural deficits in the forced swim test and in the escape/avoidance test. **a**, Fraction of immobile time over the 5 min of the forced swim test: WT, 0.12 ± 0.05 ; aLH, 0.33 ± 0.08 ; and cLH, 0.31 ± 0.05 . Results are mean \pm s.e.m.; n (number of animals) indicated in histogram bars; *, $P < 0.05$, Kruskal–Wallis test. **b**, Rate of failure to escape during 30 trials of escapable foot shock: WT, 0.12 ± 0.03 ; aLH, 0.31 ± 0.03 ; and cLH, 0.38 ± 0.05 . Results are mean \pm s.e.m.; n (number of animals) is indicated in the histogram bars; ****P* < 0.001, $F_{(2,136)} = 11.57$, one-way ANOVA. **c**, The mean frequency of mEPSCs onto VTA-projecting Lhb neurons correlates with an animal's helpless behaviour, measured as the fraction of sessions in which animals failed to escape ($R^2 = 0.69$, grey line; $P < 0.001$ by a linear regression; $n = 13$ animals; $n \geq 5$ cells for each animal). Error bars, s.e.m. **d**, The spontaneous spiking rate measured in a cell-attached configuration was higher in animals with cLH than in WT control animals: left, an example; right, histogram shows mean \pm s.e.m., and open circles are data from individual cells (WT, 0.92 ± 0.32 , $n = 17$; cLH, 3.03 ± 0.82 ; $n = 25$, **, $P < 0.01$, bootstrap).

between the Lhb and the VTA^{15,16}—are largely non-overlapping populations (Supplementary Fig. 2c), indicating that we would be able to selectively target Lhb neurons that directly project to the VTA. Lhb neurons projecting to the VTA were glutamatergic, as indicated by their co-localization with the glutamate transporter EAAC1 (also known as SLC1A1) and lack of GABAergic marker expression (Supplementary Fig. 3).

We performed whole-cell patch-clamp recordings on VTA-projecting neurons in acute parasagittal brain slices from rats that were wild-type control, had aLH or cLH (naive), or had cLH and had been exposed to mild stress (cLHms; see ‘Behavioural paradigms’ in the Methods section). We examined miniature excitatory postsynaptic currents (mEPSCs) (in the presence of tetrodotoxin to block action potentials and picrotoxin to block GABA_A-mediated synaptic currents), which were mediated by AMPA (α -amino-3-hydroxy-5-methyl-4-isoxazole propionic acid)-type glutamate receptors (Supplementary Fig. 4a) and represent responses from individual synapses onto the cells studied.

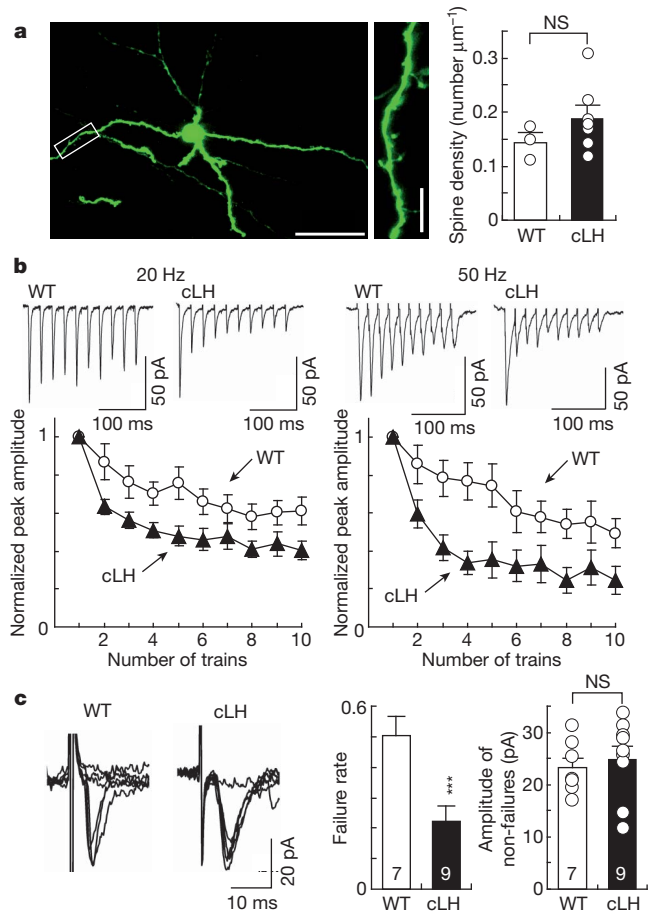


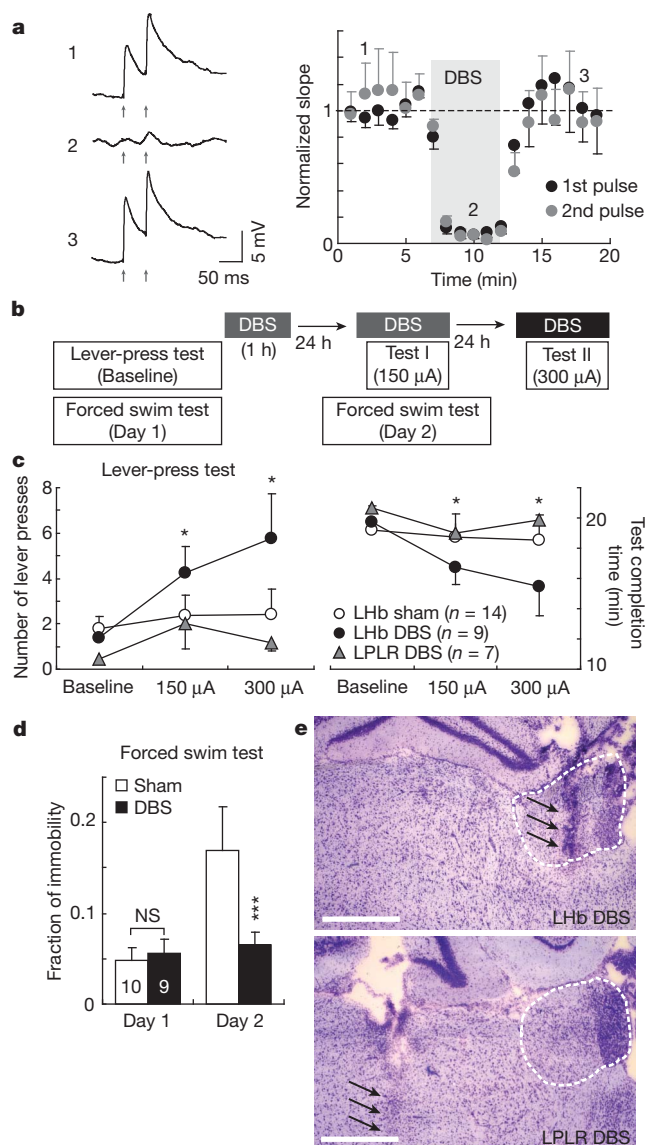
Figure 3 | Presynaptic mechanism underlying the increase in excitatory synaptic transmission onto VTA-projecting Lhb neurons in helpless animals. **a**, Two-photon laser scanning images of a VTA-projecting Lhb neuron. The neuron was labelled by *in vivo* injection into the VTA of a herpes simplex virus that expresses green fluorescent protein and is transported in a retrograde manner. The neuron is shown at low magnification (left) and high magnification (centre, image of area demarcated by white rectangle in left panel). Scale bars, 50 μ m (left) and 10 μ m (centre). Right, dendritic spine density on VTA-projecting Lhb neurons of WT animals or animals with cLH: WT, 0.15 ± 0.02 , 3 cells, 1,125.3 μ m total dendritic length; and cLH, 0.18 ± 0.02 , 7 cells, 1,002.4 μ m total dendritic length; $P > 0.1$, Student's *t*-test. **b**, Top, evoked EPSCs onto VTA-projecting Lhb neurons of WT animals or animals with cLH in response to stimulus trains (20 Hz or 50 Hz). Bottom, plot of peak EPSCs normalized to first EPSC (WT, 20 Hz $n = 10$, 50 Hz $n = 11$; and cLH, 20 Hz $n = 14$, 50 Hz $n = 13$). Compared with WT animals, animals with cLH showed a faster synaptic depression (20 Hz, $F_{(9,198)} = 2.32$, $P = 0.02$; 50 Hz, $F_{(9,198)} = 3.83$, $P < 0.001$; one-way ANOVA with repeated measures) and more extensive synaptic depression (20 Hz, $F_{(1,22)} = 6.62$, $P = 0.02$; 50 Hz, $F_{(1,22)} = 7.15$, $P = 0.01$; one-way ANOVA with repeated measures). **c**, Minimally evoked EPSCs onto VTA-projecting Lhb neurons show more failures in WT control animals than in animals with cLH (WT, 0.5 ± 0.1 , $n = 7$; cLH, 0.2 ± 0.1 , $n = 9$; ****P* < 0.001, Student's *t*-test). Mean amplitude of successful trials (right) (WT, 23.2 ± 2 , $n = 7$; cLH: 24.8 ± 2.5 , $n = 9$; $P > 0.6$, Student's *t*-test). **a–c**, Error bars, s.e.m.

The mean frequency of mEPSCs recorded from VTA-projecting Lhb neurons of rats with learned helplessness—aLH (3.7 ± 0.8 Hz (mean \pm s.e.m.), $n = 23$), cLH (4.0 ± 0.7 Hz, $n = 85$) and cLHms (4.7 ± 0.7 Hz, $n = 70$)—was higher than that of wild-type controls (2.3 ± 0.2 Hz, $n = 84$; $F_{(3,251)} = 3.1$, $P < 0.03$ comparing the wild-type control group with any other group, analysis of variance (ANOVA)) (Fig. 1a, b). In general, the distribution of mEPSC frequencies recorded across different cells in all groups had a bimodal distribution (Fig. 1c). Notably, the prevalence of neurons with high-frequency mEPSCs (>8 Hz; Fig. 1b–d, shaded region) was significantly higher

in rats with aLH (17%), cLH (14%) and cLHms (20%) than in wild-type control rats (2%; $P < 0.01$ comparing the wild-type control group with any other group, χ^2 test).

To determine whether the observed excitatory synaptic potentiation was quantitatively correlated to an animal's helpless behaviour, we first tested animals (either wild type or with cLH) by using an escape avoidance task and subsequently prepared brain slices and made recordings from the VTA-projecting neurons. For each animal, we recorded from at least five cells and plotted the mean mEPSC frequency against the animal's helpless behaviour (as measured by the fraction of trials in which the animal failed to escape from an escapable 10-s foot shock; see also Fig. 2b). The significant correlation ($R^2 = 0.69$, $F_{(1,11)} = 24.85$, $P < 0.001$, $n = 13$ for all animals; and $R^2 = 0.64$, $F_{(1,6)} = 10.7$, $P < 0.05$, $n = 8$ for animals with cLH) (Fig. 2c) indicates that the potentiation of excitatory transmission onto VTA-projecting LHB neurons is linked with an individual animal's helpless behaviour.

To examine the output of VTA-projecting neurons, we measured their spontaneous action potentials, which were more frequent in animals with cLH than in wild-type controls (Fig. 2d). We observed no differences among the various groups with respect to the amplitude of mEPSCs (Fig. 1e) or the frequency or amplitude of miniature inhibitory postsynaptic currents (Supplementary Fig. 4b, c). These results indicate that the excitatory synaptic input onto LHB neurons that project to the VTA is potentiated in the learned helplessness model.



The enhanced mEPSC frequency could result from an increase in either the number of synapses or the probability of presynaptic neurotransmitter release. To distinguish between these possibilities, we first measured the density of dendritic spines, which are the sites of excitatory synapses, on the dendrites of VTA-projecting LHB neurons. There was no significant difference in dendritic spine density between wild-type controls and animals with cLH (Fig. 3a), and there was no obvious difference in the patterns of dendritic branching between the two groups (data not shown), suggesting that there was no major difference in the number of synapses between wild-type control animals and those with cLH.

To determine whether there is a change in the efficacy of presynaptic neurotransmitter release, we examined evoked transmission. Synaptic transmission onto LHB neurons (elicited by placing a stimulating electrode in the LHB) showed distinct properties: the evoked excitatory synaptic response had a very small NMDA (*N*-methyl-D-aspartate) receptor component (Supplementary Fig. 4d), and the AMPA receptor component showed strong inward rectification (Supplementary Fig. 4e). To probe presynaptic function, we evoked transmission with high-frequency stimulation trains (ten stimuli delivered at 20 Hz or 50 Hz). The decrease in the amplitude of EPSCs in response to successive pulses during a train of stimuli reflects presynaptic vesicle depletion; more depletion correlates with a higher release probability¹⁷. VTA-projecting LHB neurons of animals with cLH showed a faster synaptic depression (at 20 Hz $F_{(9,198)} = 2.32$, $P < 0.05$; at 50 Hz $F_{(9,198)} = 3.83$, $P < 0.001$, one-way ANOVA with repeated measures) and a more extensive synaptic depression (at 20 Hz $F_{(1,22)} = 6.62$, $P < 0.05$; at 50 Hz $F_{(1,22)} = 7.15$, $P < 0.05$, one-way ANOVA with repeated measures) than those in wild-type control animals (Fig. 3b). Furthermore, with minimal stimulation, which is designed to activate few synapses (as indicated by the amplitude of non-failure responses, which is similar to the mEPSC amplitude; Fig. 3c), we measured synaptic transmission failure rate. Excitatory synaptic transmission onto VTA-projecting LHB neurons of animals with cLH had a significantly lower failure rate than that of wild-type control animals (Fig. 3c;

Figure 4 | DBS in the LHB suppresses excitatory synaptic transmission and reverses learned helplessness.

a, Left, example excitatory postsynaptic potentials (EPSPs) recorded from a VTA-projecting LHB neuron before (1), during (2) and after (3) stimulation mimicking DBS. Arrows indicate when paired pulses were given. Right, mean EPSP slope at indicated time points before, during and after DBS: (1) before (first pulse 1.1 ± 0.1 , second pulse 0.9 ± 0.1 , $n = 6$ animals); (2) during (first pulse 0.15 ± 0.07 , second pulse 0.03 ± 0.03 , $P < 0.001$ for both pulses compared with those in 1, Student's *t*-test); and (3) after (first pulse 1.2 ± 0.3 , second pulse 0.9 ± 0.2).

b, A schematic diagram showing the experimental procedures. **c**, Number of lever presses (left) and test completion time (right) for animals that received DBS or sham stimulation in the LHB or DBS in the LPLR (lateral post-thalamic nuclei, lateroventral), before (baseline) or after DBS of different intensities. For DBS in the LHB ($n = 9$), lever press baseline 1.2 ± 0.4 ; 150 μ A session 3.9 ± 1 ; and 300 μ A session ($n = 8$) 5.8 ± 2 . For DBS in the LHB ($n = 9$), test completion time baseline 19.9 ± 0.4 ; 150 μ A session 17.1 ± 1 ; 300 μ A session ($n = 8$) 15.4 ± 2 . For sham stimulation in the LHB ($n = 14$), lever press baseline 1.8 ± 0.5 ; 150 μ A session 2.4 ± 0.9 ; and 300 μ A session 2.4 ± 1 . For sham stimulation in the LHB, test completion time baseline 19.2 ± 0.5 ; 150 μ A session 18.7 ± 0.9 ; and 300 μ A session 18.5 ± 1.1 . For DBS in the LPLR ($n = 7$), lever press baseline 0.4 ± 0.2 ; 150 μ A session 2 ± 1 ; and 300 μ A session 1.1 ± 0.3 . For DBS in the LPLR, test completion time baseline 20.6 ± 0.2 ; 150 μ A session 19 ± 1.2 ; and 300 μ A session 19.9 ± 0.3 . For DBS in the LHB group, *, $P < 0.05$ compared with baseline (bootstrap). For the sham and DBS in LPLR groups, $P > 0.05$ for both measurements at both sessions compared with baseline (bootstrap).

d, Immobility during the forced swim test. For DBS, day 1, 0.06 ± 0.01 ; day 2, 0.06 ± 0.01 ; $n = 9$. For sham, day 1, 0.05 ± 0.01 ; day 2, 0.17 ± 0.05 ; $n = 10$. DBS versus sham on day 2, ***, $P < 0.001$ (bootstrap).

e, Representative cresyl violet staining of coronal brain sections after DBS in the LHB or LPLR. Arrows indicate the electrode track in the LHB (top) or LPLR (bottom). Dashed lines indicate the border of the habenula. Scale bars, 1 mm.

17. Zucker, R. S. & Regehr, W. G. Short-term synaptic plasticity. *Annu. Rev. Physiol.* **64**, 355–405 (2002).
18. Sartorius, A. & Henn, F. A. Deep brain stimulation of the lateral habenula in treatment resistant major depression. *Med. Hypotheses* **69**, 1305–1308 (2007).
19. Airan, R. D. *et al.* High-speed imaging reveals neurophysiological links to behavior in an animal model of depression. *Science* **317**, 819–823 (2007).
20. Berton, O. & Nestler, E. J. New approaches to antidepressant drug discovery: beyond monoamines. *Nature Rev. Neurosci.* **7**, 137–151 (2006).
21. Pittenger, C. & Duman, R. S. Stress, depression, and neuroplasticity: a convergence of mechanisms. *Neuropsychopharmacology* **33**, 88–109 (2008).
22. Sahay, A. & Hen, R. Adult hippocampal neurogenesis in depression. *Nature Neurosci.* **10**, 1110–1115 (2007).
23. Mill, J. & Petronis, A. Molecular studies of major depressive disorder: the epigenetic perspective. *Mol. Psychiatry* **12**, 799–814 (2007).
24. Morris, J. S. *et al.* Covariation of activity in habenula and dorsal raphe nuclei following tryptophan depletion. *Neuroimage* **10**, 163–172 (1999).
25. Roiser, J. P. *et al.* The effects of tryptophan depletion on neural responses to emotional words in remitted depression. *Biol. Psychiatry* **66**, 441–450 (2009).
26. Shumake, J. & Gonzalez-Lima, F. Brain systems underlying susceptibility to helplessness and depression. *Behav. Cogn. Neurosci. Rev.* **2**, 198–221 (2003).
27. Caldecott-Hazard, S., Mazziotta, J. & Phelps, M. Cerebral correlates of depressed behavior in rats, visualized using ^{14}C -2-deoxyglucose autoradiography. *J. Neurosci.* **8**, 1951–1961 (1988).
28. Amat, J. *et al.* The role of the habenular complex in the elevation of dorsal raphe nucleus serotonin and the changes in the behavioral responses produced by uncontrollable stress. *Brain Res.* **917**, 118–126 (2001).
29. Yang, L. M. *et al.* Lateral habenula lesions improve the behavioral response in depressed rats via increasing the serotonin level in dorsal raphe nucleus. *Behav. Brain Res.* **188**, 84–90 (2008).
30. Winter, C. *et al.* Pharmacological inhibition of the lateral habenula improves depressive-like behavior in an animal model of treatment resistant depression. *Behav. Brain Res.* **216**, 463–465 (2011).

Supplementary Information is linked to the online version of the paper at www.nature.com/nature.

Acknowledgements We thank K. Deisseroth for help and suggestions, A. Gifford and A. Biegon for sharing equipment and laboratory space, and members of the Malinow Lab and Li Lab for discussions. This study was supported by the Dana Foundation (B.L.), the Biobehavioral Research Awards for Innovative New Scientists (BRAINS) from the National Institute of Mental Health, National Institutes of Health (1R01MH091903-01) (B.L.) and the Shiley-Marcos Endowment (R.M.).

Author Contributions B.L., J.P., M.M. and C.C. contributed equally to the study. B.L., J.P., M.M., C.C., C.D.P. and D.S. performed and analysed the experiments. C.C. and B.L. made the figures. B.L., F.H. and R.M. designed the study. B.L. and R.M. wrote the manuscript.

Author Information Reprints and permissions information is available at www.nature.com/reprints. The authors declare no competing financial interests. Readers are welcome to comment on the online version of this article at www.nature.com/nature. Correspondence and requests for materials should be addressed to B.L. (bli@cshl.edu) or R.M. (rmalinow@ucsd.edu).

METHODS

Animals. Wild-type, male Sprague Dawley rats were purchased from Taconic Farms and allowed to acclimatize to the animal facility for 1–2 weeks before experiments were carried out. The cLH rats were bred as described^{11,12}. The rats were housed under a 12-h light–dark cycle (7 a.m. to 7 p.m. light), with food and water freely available. All procedures involving animals were approved by the Institute Animal Care and Use Committees of Cold Spring Harbor Laboratory, University of California, San Diego, and Brookhaven National Laboratory.

Retrograde labelling of VTA-projecting LHB neurons *in vivo*. Standard surgical procedures were followed for *in vivo* injection³¹. To label the VTA-projecting LHB neurons, we injected *in vivo* Alexa-Fluor-488-conjugated cholera toxin ($2 \mu\text{g} \mu\text{l}^{-1}$; Molecular Probes) or a herpes simplex virus expressing enhanced GFP (HSV–GFP, NeuroVex), both of which are retrograde tracers, into the VTA.

Animals were anaesthetized with isoflurane (Baxter) using an isoflurane vaporizer (Paragon Medical) and positioned in a stereotaxic apparatus that was connected to a computer system with a digital rat brain atlas (Angle Two Stereotaxic System, myNeuroLab.com). Injections of tracer solutions (3–5 injection sites along the vertical axis, 100–200 nl per injection) were delivered with a glass micropipette through a skull window ($2\text{--}3 \text{ mm}^2$) by pressure application (5–12 psi, controlled by a Picospritzer II; General Valve). The injections were performed within the following stereotaxic coordinates: -5.3 mm from bregma; 0.96 mm lateral from the midline; and $8\text{--}8.4 \text{ mm}$ vertical from the cortical surface. Rats were injected subcutaneously with 5 mg kg^{-1} carprofen (an NSAID) after surgery. During procedures, animals were kept on a heating pad and were brought back to their home cages after regaining movement. We waited 2–3 days to allow the retrograde labelling of neurons in the LHB before we killed the animals for experiments.

Preparation of acute brain slices and electrophysiology. Male rats of 40–50 days of age were used for all of the electrophysiology experiments. Animals were anaesthetized with isoflurane, decapitated and their brains quickly removed and chilled in ice-cold dissection buffer (110.0 mM choline chloride, 25.0 mM NaHCO_3 , 1.25 mM NaH_2PO_4 , 2.5 mM KCl, 0.5 mM CaCl_2 , 7.0 mM MgCl_2 , 25.0 mM glucose, 11.6 mM ascorbic acid and 3.1 mM pyruvic acid, gassed with 95% O_2 and 5% CO_2). Sagittal slices ($400 \mu\text{m}$) across the LHB were cut in dissection buffer, by using a VT1000 S vibratome (Leica), and subsequently transferred to a storage chamber containing artificial cerebrospinal fluid (ACSF) (118 mM NaCl, 2.5 mM KCl, 26.2 mM NaHCO_3 , 1 mM NaH_2PO_4 , 20 mM glucose, 4 mM MgCl_2 and 4 mM CaCl_2 , at $22\text{--}25^\circ\text{C}$, pH 7.4, gassed with 95% O_2 and 5% CO_2). After at least 1 h recovery time, slices were transferred to the recording chamber and were constantly perfused with ACSF maintained at 27°C .

Experiments were always performed on interleaved wild-type control and cLH or aLH animals. About three-quarters of the experiments were carried out blinded to the experimental group. These showed the same results as the non-blinded experiments, and the data were combined. Whole-cell patch-clamp recordings were obtained with Axopatch-1D amplifiers (Axon Instruments) onto neurons in the LHB under visual guidance using transmitted light illumination. For evoked EPSCs, synaptic transmission was evoked with a bipolar stimulating electrode placed close to the stria medullaris, typically $>0.2 \text{ mm}$ away from cell bodies. Responses were recorded at holding potentials of -60 mV (for AMPA-receptor-mediated responses) and $+40 \text{ mV}$ (for detection of any NMDA-receptor-mediated responses and measurement of rectification). NMDA-receptor-mediated responses were quantified as the mean current between 110 ms and 160 ms after stimulation. Bathing solution (ACSF) contained 119 mM NaCl, 2.5 mM KCl, 2 mM CaCl_2 , 1 mM MgCl_2 , 26.2 mM NaHCO_3 , 1 mM NaH_2PO_4 , 11 mM glucose, and 0.1 mM picrotoxin, gassed with 5% CO_2 and 95% O_2 , at 27°C (unless otherwise noted). Internal solution for voltage-clamp experiments contained 115 mM caesium methanesulphonate, 20 mM CsCl, 10 mM HEPES, 2.5 mM MgCl_2 , 4 mM $\text{Na}_2\text{-ATP}$, 0.4 mM Na-GTP, 10 mM Na-phosphocreatine and 0.6 mM EGTA (pH 7.2). Spermine ($100 \mu\text{M}$) was included in the internal solution for measurement of rectification. mEPSCs were recorded at 27°C in the presence of $1 \mu\text{M}$ tetrodotoxin (TTX) and $100 \mu\text{M}$ picrotoxin in sagittal slices and analysed using Mini Analysis Program (Synaptosoft). To isolate miniature inhibitory spontaneous responses (mIPSCs), $1 \mu\text{M}$ TTX, $100 \mu\text{M}$ APV (D-(–)-2-amino-5-phosphonopentanoic acid) and $3 \mu\text{M}$ NBQX were added.

For the experiments in which high-frequency stimulation trains were used to determine presynaptic release probability, QX314 (5 mM) was included in the internal solution to prevent the generation of sodium spikes. To recruit the maximal number of axon terminals that can be stimulated by the high-frequency trains, thereby minimizing the effects of axonal failures and reducing the variability in responses, a low concentration (100 nM) of NBQX was included in the bath ACSF. This allowed stimulation at a higher intensity without evoking large EPSCs that could activate voltage-dependent conductances. For experiments testing the effects of DBS on synaptic transmission onto VTA-projecting LHB neurons, evoked EPSCs were monitored before, during and after a stimulation protocol mimicking

clinical DBS. Stimulation consisted of episodes of 44 trains of stimuli separated by 40 ms. During each train, seven stimuli were applied at a frequency of about 130 Hz. The inter-episode interval was 200 ms, during which two stimuli separated by 50 ms were applied to monitor the amplitude and slope of the EPSP. The DBS protocol and the paired-pulse stimulation were delivered using the same electrode.

Two-photon imaging of dendritic spines. Image acquisition and analysis were described previously^{32,33}. Images were acquired on a custom built dual channel two-photon laser scanning microscope (based on the Olympus FluoView laser scanning microscope) using a Ti:Sapphire Chameleon laser (Coherent), which was mode locked to 910 nm. Full three-dimensional (3D) image stacks were acquired using a $\times 60$ 0.9 NA objective lens at $\times 5$ digital zoom (FluoView software, Olympus), 70 nm per pixel. Each image plane was resampled three times and spaced $0.5 \mu\text{m}$ in the z dimension.

Behavioural paradigms. Methods for the learned helplessness paradigm have been optimized previously³⁴. To prepare animals with learned helplessness (the aLH group) for behavioural testing and electrophysiological recording, rats were exposed to a learned helplessness ‘training session’ 5 days after *in vivo* injection of retrograde tracers into the VTA. This session consisted of 120 inescapable, uncontrollable electric foot shocks at 0.8 mA over 40 min in the shocking chambers (Coulbourn Instruments; chambers were 12 inches wide \times 10 inches deep \times 12 inches high and were controlled by precision adjustable shockers), with random shock duration ranging from 5 s to 15 s and unpredictable inter-shock intervals (ITIs). Experiments were performed on pairs of littermates housed in the same cage. Control animals were placed in the shocking chamber in parallel for 40 min, without being shocked. Electrophysiological recordings on acute brain slices were performed 24–48 h after shocking. Animal identity was coded for blinding the researcher with respect to treatment. To prepare cLH animals exposed to mild stress (the cLHms group), cLH rats were treated with a procedure essentially the same as the active avoidance task (see below), during which animals received an average of 152 ± 27 s of escapable foot shock ($n = 8$), and acute brain slices were prepared after 2 h.

To evaluate learned helplessness behaviour, we used both a lever-pressing task and an active avoidance task. The lever-pressing task was described previously³⁴. Briefly, an illuminated lever was added to the shocking chamber in the testing session, which comprised 15 escapable foot shocks lasting up to 60 s (shorter if terminated by a lever press) over 21 min, and with fixed ITIs of 24 s. The active avoidance task was performed in a shuttle box (20 inches wide \times 10 inches deep \times 12 inches high; Coulbourn Instruments) equipped with an electrical grid floor, a door separating the two halves, and photocell detectors. The shuttle box was placed in a sound-attenuating chamber to minimize external stimuli. Testing was fully automated using Graphic State software (Coulbourn Instruments). Animals were allowed to explore the shuttle box for 5 min, and helpless behaviour was evaluated over 30 trials of unexpected and escapable foot shock (1.2 mA intensity, 10 s duration, with random ITIs of 24 ± 12 s) following a 5-s cue tone. Foot shock was terminated if the animal completely crossed to the other side of the cage. When an animal crossed the cage during the 5-s cue tone presentation, avoidance was scored. If an animal crossed during the 10-s shocks, the mean escape latency was measured. Failure was recorded if no crossing was made during the 10-s shock.

For the forced swim test, animals were forced to swim for 5 min in a cylinder of water (water temperature was $25\text{--}26^\circ\text{C}$; the cylinder was 30 cm in diameter and 40 cm high; the depth of the water was set to prevent animals from touching the bottom with their hind limbs). Animal behaviour was videotaped using a PC6EX3 infrared camera (SuperCircuits). The immobile time each animal spent during the test was manually counted offline, with the evaluator being blind to the treatment of the animals.

Deep brain stimulation (DBS). To prepare animals with learned helplessness for the DBS experiments, animals were first treated with a ‘training’ session and then 24 h later, a ‘testing’ session, as described above. On the basis of the test results, animals that met the criteria (those that pressed the lever only 0–5 times, and took between 16 and 21 min to finish the test) were used to test the effects of DBS. For increased stringency, only lever presses occurring within the first 20 s of shock onset were counted. Fifty two male Sprague Dawley rats were trained and tested, and 26 of these animals met the criteria. Three days later, standard surgical procedures were used to implant bipolar concentric electrodes (8 mm long, 0.8 mm tip diameter; Plastics One) unilaterally into the LHB (coordinates -3.7 mm AP , $\pm 0.7 \text{ mm ML}$ and -5.4 mm DV) in rats that met the criteria.

After 3–5 days recovery from surgery, rats underwent a training session followed by a ‘baseline’ learned helplessness test. Three animals, in which the electrodes were implanted into the LHB, were excluded from further study because their performance did not meet the criteria during the baseline test. Immediately following the baseline test, DBS (seven stimulus trains of 130 Hz, separated by 40 ms intervals; $150 \mu\text{A}$ intensity) in the LHB or the thalamus, or no stimulation (sham), was applied for 1 h. Twenty-four hours later, another 1-h session of DBS

or sham stimulation was given immediately before and during the learned helplessness test. DBS intensity was 150 μ A. Another 24 h later, the final 1-h session of DBS (or sham stimulation) was given at a higher intensity (300 μ A), immediately before and during the final learned helplessness test (see Fig. 4b for a schematic diagram showing the experimental procedures). Only animals with the electrode correctly placed in the LHb or thalamus (LPLR) were included for the respective behavioural analysis.

To test the effects of DBS on the forced swim test, electrodes were implanted in the same way as described above, except that in the DBS group two rats had bilateral implants and that in the sham group three rats had bilateral implants. The rest of the animals had unilateral implants (total animals used for the forced swim test: DBS $n = 9$ and sham $n = 10$). Immobility time was recorded during the first 5 min of a 15-min swimming session on day 1. DBS (150 μ A) or sham stimulation was applied for 1 h following the forced swim test on day 1. Twenty-four hours later (day 2), another 1 h of DBS (150 μ A) or sham stimulation was applied, and immobility time was recorded during the 5-min swimming session.

To determine the volume of tissue affected by DBS in the LHb, in a separate set of experiments, animals were perfused with 4% PFA 2 h after the onset of DBS, and brains were processed for immunohistochemistry to examine Fos expression.

Immunohistochemistry. Immunohistochemistry experiments were performed following standard procedures on 50- μ m brain sections fixed with 4% PFA. The

antibodies used were anti-NeuN antibody (Chemicon), anti-EAAC1 antibody (Chemicon), anti-GABA antibody (Sigma), anti-GAD67 antibody (Chemicon) and anti-Fos antibody (Santa Cruz Biotechnology). After finishing the immunohistochemistry process, images were taken using either an LSM 510 confocal microscope (Zeiss; for double labelling with two colours) or a BX41 histology microscope (Olympus; for single labelling with one colour), using $\times 20$ objectives.

Statistics and data presentation. To compare the means of non-normally distributed data sets, we used a bootstrap procedure. Two data sets (N and M of size n and m) were randomly sampled n and m times, respectively, allowing resampling, and means (N_i and M_i) were generated. This procedure was repeated 10,000 times. If N_j was more than M_j fewer than 5% of the times, then the probability that N is more than M was estimated to be less than 0.05. Similar calculations established probabilities less than 0.01. All other statistical tests are indicated when used. All data are presented as mean \pm s.e.m.

31. Rumpel, S., LeDoux, J., Zador, A. & Malinow, R. Postsynaptic receptor trafficking underlying a form of associative learning. *Science* **308**, 83–88 (2005).
32. Kopec, C. D. *et al.* Glutamate receptor exocytosis and spine enlargement during chemically induced long-term potentiation. *J. Neurosci.* **26**, 2000–2009 (2006).
33. Kopec, C. D., Real, E., Kessels, H. W. & Malinow, R. GluR1 links structural and functional plasticity at excitatory synapses. *J. Neurosci.* **27**, 13706–13718 (2007).
34. Vollmayr, B. & Henn, F. A. Learned helplessness in the rat: improvements in validity and reliability. *Brain Res. Brain Res. Protoc.* **8**, 1–7 (2001).